Could Compton scattering be used for measuring the beam energy at the International Linear Collider?

Hannu Paukkunen

Jyväskylä university, Department of Physics
PL 35 (YFL) 40014 JYVÄSKYLÄN YLIOPISTO, Finland
Email: htpaukku@st.jyu.fi

In this report we study the feasibility of precise beam energy measurements based on the inverse Compton scattering in the context of the International Linear Collider. Basically the method needs the measurement of a magnetic field integral and the bending angles of the electrons in the Compton edge region. We show, by solely kinematical arguments, that the precision requirement $\Delta E_{\mathrm{beam}}/E_{\mathrm{beam}} = 10^{-4}$ can be satisfied with a low energy CO_2-laser with a photon energy of $E_{\mathrm{laser}} = 0.117\,\mathrm{eV}$, provided the positions of the scattered photons and edge electrons can be determined within some micrometers. For reliable measurements the number of Compton events for each electron bunch should be statistically significant. Our analysis taking into account the cross-section and luminosity implies that this should be possible with a suitably chosen pulsed laser with a pulse energy of $10 - 100\,\mu\mathrm{J}$.

1 Introduction

The precise knowledge of the beam energy is an essential piece of information for successful experiment in the high energy physics. This would be especially true for the International Linear Collider (ILC) — an $e^- e^+$-machine planned to be built to make precision measurements in close interplay with the LHC in an energy range between the Z-pole and $500\,\mathrm{GeV}$.

The precision knowledge of E_{beam} and hence $\sqrt{s}$ is in particular importance for two types of experiments: treshold scans and and reconstructions of particle resonances. For instance, measuring the $\sqrt{s}$ dependence of the $t\bar{t}$-pair production cross-section near its production treshold is a way to determine the top quark mass M_{top} accurately. To measure the top quark mass within $\Delta M_{\mathrm{top}} < 100\,\mathrm{MeV}$ demands the beam energy to be known with a relative accuracy of 10^{-4}.

It would be advantageus to have two complementary measurements for the beam energy so that the cross-check would be possible. Several proposed techiques for determining the beam energy exists. For example, one of the most promising is based on an accurate measurement of the beam position in a magnetic chicane [1] and synchroton radiation based method [2]

could also be possible. For other methods see ref. [1] and references therein.

In this report we study the feasibility of measuring the ILC beam energy using *inverse Compton scattering*. Similar studies, but for significantly lower beam energies, can be found from [3].

2 Basic principle

Compton scattering is an elastic process between a photon and an electron

$$ e^- + \gamma \rightarrow e^- + \gamma. \tag{1} $$

Usually, in Compton scattering the electron is intially at rest and receives a part of the colliding photon's energy and momentum. In the inverse Compton scattering process the photon scatters off from a high energy electron and the direction of the energy-momentum transfer is opposite. This is the basic idea behind the method we are now going to describe.

The conceptual sketch of the experimental setup is shown in fig. (1). When the ultra relativistic beam electrons interact with the laser photons some of their energy and momentum is transfered to the outgoing photons. The vast
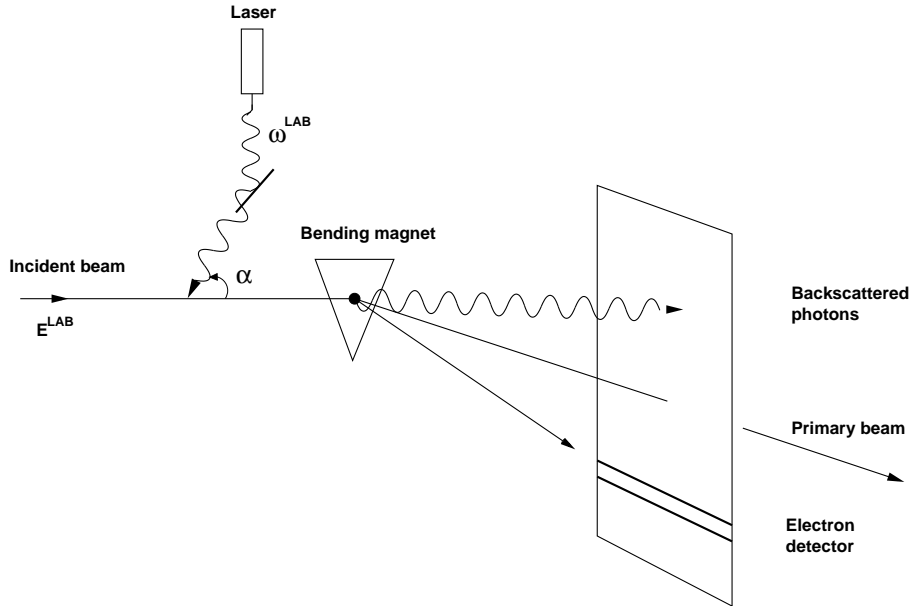
Fig. 1: *Experimental setup. The energies of colliding electrons and photons are E^{LAB} and ω^{LAB}, respectively, and α is the crossing-angle.*

majority of the beam electrons, however, remain unchanged after crossing with the laser but are thereafter accompanied by the scattered photons and electrons. The energies of the scattered electrons lie in a certain range $E_{\text{edge}}...E^{\text{LAB}}$ where the minimum energy E_{edge} follows from the energy-momentum conservation and it is given by

$$E_{\text{edge}} = \frac{E^{\text{LAB}}}{1+k}, \qquad (2)$$
$$k = \frac{2\gamma\omega^{LAB}\,(1+\cos\alpha)}{m},$$

where $\gamma = m/E^{\text{LAB}}$ is the Lorentz factor for the electron and the other variables are indicated in fig. (1). This is known as the *Compton edge*.

Due to the high momentum of the electron beam the scattered particles are strongly collimated in the forward direction and in order to separate the scattered electrons from the primary beam we need a bending magnet. The relation between the bending angle Θ and energy E of an ultra relativistic electron in a magnetic field B is

$$\Theta = \frac{c \cdot e}{E} \int_{\text{magnet}} B d\ell, \qquad (3)$$

where e is the unit charge, c is the speed of light and the integration is performed along the trajectory of the electron within the B-field. From

this equation we note that the scattered electrons provide a continuous pattern in the detector which is terminated by a sharp edge due to the lowest energy electrons at the Compton edge. The back-scattered photons are not deflected by the magnetic field and hit the detector with the center-of-gravity pointing the direction of the original electron beam.

If the distance between the magnet and the detector is known, measuring accurately the distance between the Compton edge and the center-of-gravity of the back-scattered photons would allow the determination of the bending angle and eventually the beam energy via equations (2) and (3).

3   Kinematics

The cross-section for the Compton scattering is most easily calculated in the electron rest-frame and a transformation between the laboratory (LAB) frame and the rest frame of the electron is needed. These frames are shown in fig. (2) where also some kinematical quantities are indicated. Beginning from the LAB-frame the electron rest frame is reached by a Lorentz boost along the z-axis. This results with a photon energy

$$\omega = \gamma\omega^{LAB}(1+\cos\alpha). \qquad (4)$$

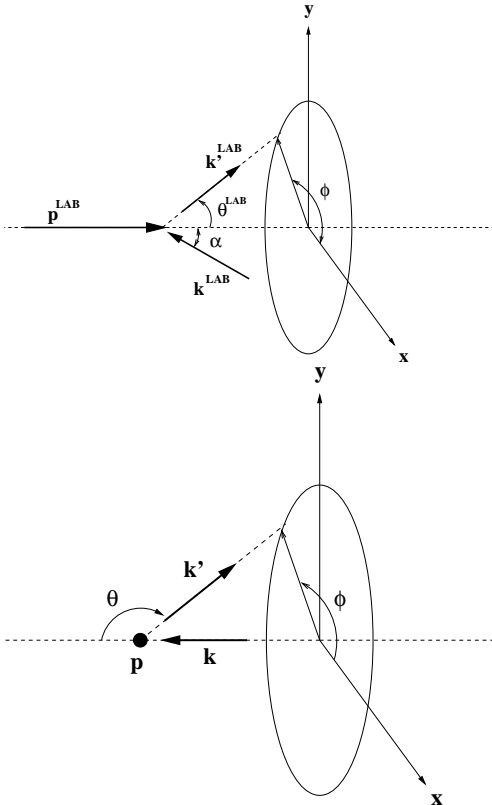Fig. 2: *The two frames*

Since the crossing angle α is suppressed by the boost with a factor of γ^{-1}, we can safely neglect α hereafter and write the four-momenta for the particles involved as

$$
\begin{aligned}
p &= (m, 0, 0, 0) \\
k &= (\omega, 0, 0, \omega) \\
k' &= \omega'(1, \sin\theta\cos\phi, \sin\theta\sin\phi, \cos\theta) \\
p' &= p + k - k'.
\end{aligned}
$$

Since all particles are on-shell we have

$$
\begin{aligned}
m^2 &= p'^2 = (k + p - k')^2 \\
&= k^2 + p^2 + k'^2 + 2p \cdot (k - k') - 2k \cdot k' \\
&= m^2 + 2m(\omega - \omega') - 2\omega\omega'(1 - \cos\theta),
\end{aligned}
$$

so that ω', the scattered photon energy, is

$$
\omega' = \frac{\omega}{1 + (1 - \cos\theta)\omega/m} \tag{5}
$$

which relates the photon energy and scattering angle θ. This is the Compton's famous formula [4]. Boosting the four-veector k' back to the

LAB-frame results

$$
\begin{aligned}
\omega'^{\text{LAB}} &= \gamma\omega'(1 - \cos\theta) & (6) \\
\tan\theta^{\text{LAB}} &= \frac{\sin\theta}{\gamma(\cos\theta - 1)}. & (7)
\end{aligned}
$$

Due to energy-momentum conservation this is sufficient to fix the energy and the scattering angle of the final state electron. In the fig. (3) we show the behaviour of the electron and the photon angles against their scattering energies in the LAB-frame confirming our statement about very small angular spread.

The minimum of E'^{LAB} (maximum of ω'^{LAB}) occurs when $\theta = \pi$ which corresponds to the edge energy of the electrons given by eq. (2). The behaviour of this edge is of a great importance and in figure (4) it is shown how the edge behaves as a function of beam energy. It clearly reveals that as the energy of the laser photons grows the edge energy becomes nearly constant. In such a situation it eventually becomes impossible to resolve beam energy variations! The reason can be easily understood if we rewrite the edge energy as

$$
E_{\text{edge}} = \frac{1}{1/E^{\text{LAB}} + 2\omega^{\text{LAB}}(1 + \cos\alpha)/m^2}.
$$

In the limit of $E^{\text{LAB}} \to \infty$, E_{edge} becomes constant and the only way to retain some beam energy sensitivity is to reduce ω^{LAB}.
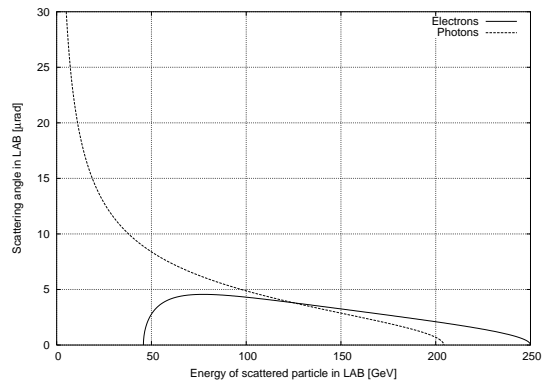

Fig. 3: *Scattering angles versus the energy of the scattered photon and electron in a LAB-frame for a beam energy of 250 GeV, a Nd:YAG laser with energy 1.165 eV and, a crossing-angle $\alpha = 10\ mrad$.*

The most demanding point is the measurement of the distance d between the center-of-gravity of the back-scattered photons and the electron edge with a sufficient precision. We estimate the needed accuracy Δd in the following

Tab. 1: *Values of (d, Δd) pairs for typical laser energies. Two lengths for the lever arm and two bending angle values are considered.*

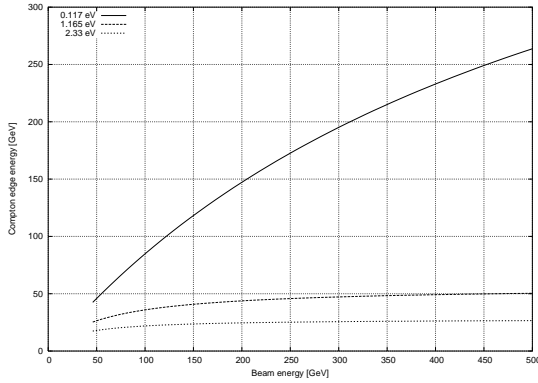| Laser energy	Bending angle 0.5 mrad		Bending angle 1 mrad	
	30m	50m	30m	50m
0.117 eV	$2.1cm, 1.5\mu m$	$3.6cm, 2.5\mu m$	$4.3cm, 3.0\mu m$	$7.2cm, 4.9\mu m$
1.165 eV	$8.2cm, 1.3\mu m$	$14cm, 2.1\mu m$	$16cm, 2.5\mu m$	$27cm, 4.2\mu m$
2.33 eV	$15cm, 0.18\mu m$	$25cm, 0.31\mu m$	$30cm, 0.36\mu m$	$50cm, 0.61\mu m$

Fig. 4: *Compton edge energy as a function of the beam energy for different energies of the laser photons. Angle $\alpha = 10$ mrad, and the laser energies correspond the available CO_2-laser (0.117 eV) and Nd:YAG laser (1.165 eV, 2.33 eV)*

Fig. 5: *An example of experimental parameters.*

way: From eq. (2) we get

$$\frac{\Delta E_{\text{edge}}}{E_{\text{edge}}} = \frac{E_{\text{edge}}}{E_{\text{beam}}} \times \frac{\Delta E_{\text{beam}}}{E_{\text{beam}}}, \qquad (8)$$

which is related to the accuracy of magnetic field and bending angle via eq. (3)

$$\left(\frac{\Delta E_{\text{edge}}}{E_{\text{edge}}}\right)^2 = \left(\frac{\Delta \Theta}{\Theta}\right)^2 + \left(\frac{\Delta B}{B}\right)^2 \qquad (9)$$

On the other hand, from the geometry of the setup $d = \Theta L$ and thus

$$\left(\frac{\Delta \Theta}{\Theta}\right)^2 = \left(\frac{\Delta d}{d}\right)^2 + \left(\frac{\Delta L}{L}\right)^2. \qquad (10)$$

Hence, the relative error of d can be expressed as

$$\left(\frac{\Delta d}{d}\right)^2 = \left(\frac{E_{\text{edge}}}{E_{\text{beam}}}\frac{\Delta E_{\text{beam}}}{E_{\text{beam}}}\right)^2 \qquad (11)$$
$$- \left(\frac{\Delta B}{B}\right)^2 - \left(\frac{\Delta L}{L}\right)^2$$
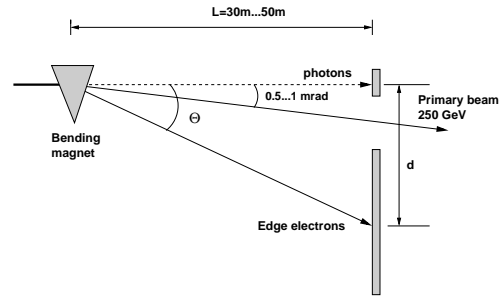
Let us consider the special case of a 250 GeV primary beam which is deflected by an angle of 0.5...1 mrad as shown in fig. (5). We demand

$$\Delta E_{\text{beam}}/E_{\text{beam}} = 10^{-4},$$

and assume

$$\Delta B/B = 1 \cdot 10^{-5}$$
$$\Delta L = 10\mu m,$$

where $B \equiv \int B d\ell$. We obtain the accuracies needed for d, shown in tab. (1).

This example gives the size of the required accuracy of Δd. For laser energies below 2 eV Δd lies in the region of few μm and for more energetic lasers it drops below 1 μm. Therefore, lasers with photon energy below 1.2 eV are preferable for our purposes.

As we go to the 500 GeV beam energy the demands for Δd become even more stringent. From the lasers considered above only the CO_2-laser with a photon energy of 0.117 eV can provide the required accuracy for the beam energy, with Δd still in the few μm region. However, it should be noted that these numbers are quite sensitive to the acccuracy of the field integral $\int B d\ell$ and any improvement of this quantity would reduce the needed accuracy for d.

In reality the scattered electron edge in the detector is not sharp but somewhat smoothed

and to achieve high precision requires sufficient statistics. To make an estimation we need to calculate the cross-section and expected luminosity for the Compton process.
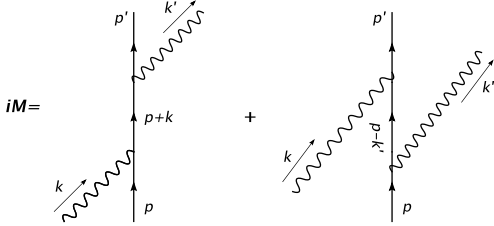
4 Compton cross-section

Fig. 6: *Leading order graphs contributing to the Compton cross-section*

To leading order (Born approximation), the matrix element for Compton scattering consists of two Feynman graphs shown in fig. (6). At some stage, the ILC is planned to run with polarized electrons/positrons, so that we have to account for the possible spin-states of the electron in our calculation. To optimize the cross-section, it turns out that it is also advantageous to fix the photon polarization. The spin and polarization states of the final electron and photon are not interesting and are summed over. Using the Feynman rules for QED the matrix element for the Compton process reads

$$
\begin{aligned}
i\mathfrak{M} &= \overline{u}(p',s')\left(-ie\gamma^{\mu}\right)\epsilon_{\mu}^{*\,\prime}\frac{i\left(\not{p}+\not{k}+m\right)}{(p+k)^2-m^2} \\
&\quad (-ie\gamma^{\nu})\,\epsilon_{\nu}u(p,s) \\
&+ \overline{u}(p',s')\left(-ie\gamma^{\nu}\right)\epsilon_{\nu}\frac{i\left(\not{p}-\not{k}'+m\right)}{(p-k')^2-m^2} \\
&\quad (-ie\gamma^{\mu})\,\epsilon_{\mu}^{*\,\prime}u(p,s).
\end{aligned}
$$

Now, this should be squared and summed over the final particles' polarization and spin states. In order to reduce the calculation to traces of γ-matrices one should use the spin projection operator

$$
\Sigma(s) = \frac{1}{2}\left(1+\gamma^5\not{s}\right) \tag{12}
$$

in front of $u(p,s)$ so that the summation over initial spin states can formally be done without getting contribution from the wrong spin states. The explicit calculation is quite involved and far too lengthy to present here and we merely quote

Tab. 2: *Varibles specifying the polarizations in the cross-section formula*

Photon polarization	P_L	P_C
Left handed	0	−1
Right handed	0	+1
Linearly polarized	+1	0
Unpolarized	0	0
Electron polarization	S_T	S_L
+z-direction	0	+1
-z-direction	0	−1
Transversely polarized	+1	0
Unpolarized	0	0

the results:

$$
\frac{d\sigma}{d\Omega} = \frac{\hbar^2 c^2 \alpha_F^2}{2m^2}\left(\frac{\omega'}{\omega}\right)^2 \tag{13}
$$
$$
\left[\Sigma_0 + P_L\Sigma_1 + P_C\left(\Sigma_{2T}+\Sigma_{2L}\right)\right]
$$

where

$$
\begin{aligned}
\Sigma_0 &= \frac{\omega'}{\omega}+\frac{\omega}{\omega'}-\sin^2\theta \\
\Sigma_1 &= -\sin^2\theta\cos 2\left(\phi-\eta\right) \\
\Sigma_{2T} &= -S_T\left(1-\frac{\omega'}{\omega}\right)\sin\theta\cos(\phi-\xi) \\
\Sigma_{2L} &= -S_L\left(\frac{\omega}{\omega'}-\frac{\omega'}{\omega}\right)\cos\theta,
\end{aligned}
$$

and α_F is the Sommerfeld fine structure constant. Possible values for the electron and photon polarizations are summarized in table (2). The angles η and ξ specify the azimuthal angles of the linear polarized photons and transverse polarized electrons, respectively. All quantities are given in the electron rest frame. Note that in the unpolarized case only Σ_0 contributes and the cross-section equals the famous Klein-Nishina formula [5]! Our results have been cross-checked against the formulas given in the literature [6, 7].

When analysing Compton scattering of ultra relativistic electrons it is useful to consider the cross-section behaviour as a function of the energy of the scattered electrons. This can be achieved by means of the relation

$$
\cos\theta = \frac{E^{LAB}-\left(1+\frac{2}{k}\right)\omega'^{LAB}}{E^{LAB}-\omega'^{LAB}}, \tag{14}
$$

which follows straightforwardly from eq. (6), (5) and (4). Fig. (7) shows the behaviour of the differential cross-section $d\sigma/dE'^{LAB}$ after integration over the azimuthal angle ϕ for the most important polarization configurations. Note that after integration over ϕ the contribution of Σ_1 and Σ_{2T} vanish. This means that if the laser is linear polarized or the polarization of the electron is transverse, the cross-section coincides with the unpolarized case! In fig. (8) the total cross-section for the unpolarized situation is shown. From figures (7) and (8) we can
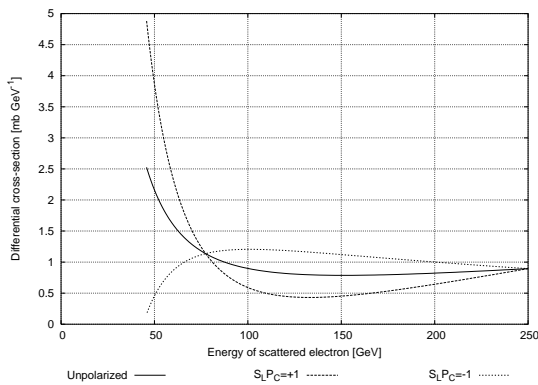

Fig. 7: *Differential cross-section for a beam energy* 250 GeV *and* 1.165 eV *laser energy with a crossing angle* $\alpha = 10$ mrad. *The different initial polarization states are indicated.*

draw some conclusions:

- The cross-section peaks at the Compton edge which is advantageous for the precise determination of the distance d

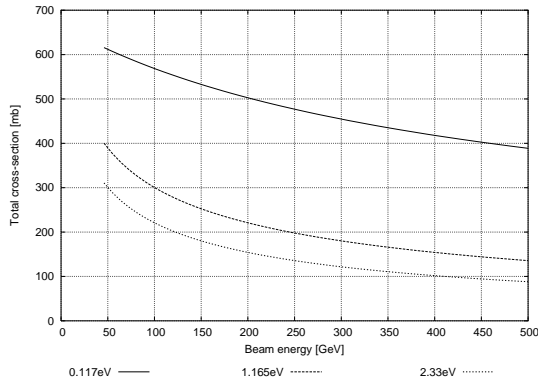- Choosing the laser with wrong circlar polarization can spoil the method

Fig. 8: *The total Compton cross-section for the unpolarized case for various laser energies. A crossing angle of* $\alpha = 10$ mrad *is assumed.*

- Low-energy lasers are advantageous also from the point of view of having higher cross-sections

5 Luminosity

To turn the cross-section to number of Compton scattering events we need to know the luminosity $\mathfrak{L}$ for $e^-\gamma$-collisions. In principle, there are two possibilities: One is to shine the electron beam with a continuous laser and the other one is to have a pulsed laser that matches the pattern of e^--bunches in the beam. In the formulae that follows the particle densities in the beam are assumed to be Gaussian-shaped and the full derivation can be found in ref. [8].

- Continuous laser

The luminosity per electron bunch is given as

$$\mathfrak{L}_{\text{cont}} = \frac{1 + \cos\alpha}{\sqrt{2\pi}\sin\alpha}\frac{N_e P_L}{c\,E_{\text{laser}}}\frac{1}{\sqrt{\sigma_{x\gamma}^2 + \sigma_{xe}^2}}$$

Here N_e is the number of electrons in a bunch, P_L is the average power of the laser with photon energy E_{laser}, and α is the crossing angle between the two beams. The horizontal beam sizes are characterized by $\sigma_{x\gamma}$ and σ_{xe}.

As the crossing-angle α becomes zero the expression above explodes. However, assuming that the electron bunches are completely inside the laser spot the luminosity is limited by the laser beam finite emittance ε_γ [9] given by

$$\mathfrak{L}_{\text{cont,max}} = \frac{N_e P_L}{c\,E_{\text{laser}}}\frac{1}{\varepsilon_\gamma}. \qquad (16)$$

For a perfect laser the minimum emittance is $\varepsilon = \lambda/(4\pi)$ and restricts the highest possible luminosity to

$$\mathfrak{L}_{\text{cont,max}} = 4\pi\frac{N_e P_L}{hc^2}. \qquad (17)$$

where h is the Planck constant and c is the speed of light.

- Pulsed laser

The Luminosity per bunch crossing is given as

$$\mathfrak{L}_{\text{pulsed}} = N_\gamma N_e g \qquad (18)$$

N_γ denotes the number of photons per laser pulse and g is a geometrical factor given by eq.

$$g = \frac{\cos^2 \alpha/2}{2\pi} \frac{1}{\sqrt{\sigma_{xe}^2 + \sigma_{x\gamma}^2}} \frac{1}{\sqrt{\left(\sigma_{ye}^2 + \sigma_{y\gamma}^2\right)\cos^2(\alpha/2) + \left(\sigma_{ze}^2 + \sigma_{z\gamma}^2\right)\sin^2(\alpha/2)}} \quad (15)$$

Tab. 3: *Parameters for estimating the luminosity.*

N_e	2×10^{10}
Bunch spacing	$337\,\mathrm{ns}$
Bunch length	$300\mu\mathrm{m}$, 1 ps
Horizontal beam size	$\sigma_{xe} = 10\mu\mathrm{m}$
Vertical beam size	$\sigma_{ye} = 2\mu\mathrm{m}$
Laser beam size	$\sigma_{x\gamma} = \sigma_{y\gamma} = 40\mu\mathrm{m}$
Crossing angle	$\alpha = 10\,\mathrm{mrad}$

Tab. 4: *Number of events corresponding to one electron bunch for a continuous and a pulsed lasers. For the continuous laser the number of events are normalized to the average power of the laser, while for the pulsed laser the normalization is to the total pulse energy.*

Continuous	Events/P_L $[W^{-1}]$		
laser	$1.165\,\mathrm{eV}$	$2.33\,\mathrm{eV}$	$0.117\,\mathrm{eV}$
	0.014	0.0047	0.3
Laser pulse	Events/E_P $[(\mu J)^{-1}]$		
length	$1.165\,\mathrm{eV}$	$2.33\,\mathrm{eV}$	$0.117\,\mathrm{eV}$
1 ns	5.5	1.9	130
100 ps	53	18	1300
10 ps	190	65	4600

(15). In this case also the verical sizes $\sigma_{y\gamma}$, σ_{ye} and the longitudinal sizes $\sigma_{z\gamma}$, σ_{ze} contribute.

To get some numbers out of the equations we first fix some parameters of the laser and electron beams, see tab. (3). With the total cross-section in our hand we calculate the number of events for each e^- bunch normalized to the average power of the laser P_L or to the total pulse energy E_P for continuous and pulsed lasers respectively.

The results are shown in tab. (4). In order to estimate the number of Compton events needed to resolve the Compton edge in a reliable manner, a dedicated simulation is needed. At this stage we just guess that the number of events should be in the order of 10^4. This rules out the use of a continuous laser but for a pulsed laser the situation is not as bad.

The DESY TTF facility [10] has already developed a laser that is able to deliver $1.18\,\mathrm{eV}$ photons in a 10 ps pulse length at a $3\,\mathrm{MHz}$ rate, with a pulse energy up to $140\mu J$. This brings the number of Compton events expected close to the needed level. A pulsed CO_2 laser that would satisfy our demands needs a significantly lower pulse energy.

Furthermore, the Laser-Based Beam Diagnostics (LBBD) Collaboration is developing laser-based techniques to determine the transverse dimensions of electron (positron) bunches at the ILC. They are aiming for a pulsed laser with a pulse energy in the mJ region which would also match the bunch pattern at the ILC. Although the laser energy envisaged is in the visible region of $2.33\,\mathrm{eV}$, a variant of such a laser could be suited for our purpose.

6 Conclusions

We have considered the feasibility of using the inverse Compton scattering as a tool for measuring the beam energy at the ILC. First of all, the method is simple requiring only one bending magnet and a high-resolution position detector for electrons and photons. It is also non-destructive to the electron beam since only a small fraction of the electrons in a bunch are needed for the measurement.

We have demonstrated that purely kinematical arguments are quite restrictive to the properties of the laser with respect to the photon energy. With a laser photon energy of $E_{\mathrm{laser}} < 1.2\,\mathrm{eV}$ and $\Delta B/B \sim 10^{-5}$, a relative precision 10^{-4} for the beam energy around $250\,\mathrm{GeV}$ requires position measurements of the back-scattered photons and the edge electrons within some micrometers. At $500\,\mathrm{GeV}$ however, a similar accuracy needs to improve either the accuracy of magnet field integral and/or lowering the laser energy down to the CO_2 level of $E_{\mathrm{laser}} = 0.117\,\mathrm{eV}$.

Our calculations on cross-sections and luminosities also prefer the use of lasers with $E_{\mathrm{laser}} < 1.2\,\mathrm{eV}$. In addition, the laser should be pulsed

matching the $3\,\mathrm{MHz}$ pattern of the e^--bunches in the ILC beam. We estimate, that with a pulse length of $10\,\mathrm{ps}$ the laser should have at least a $10...100\mu\mathrm{J}$ pulse energy to provide enough events for a reliable position measurement of the scattered photons and electrons. A laser operating with $1.18\,\mathrm{eV}$ of photon energy would satisfy our requirements and, fortunately, such as laser already exists. Also, R & D for similar lasers needed for other purposes related to the ILC is ongoing. For our demands, however, a pulsed laser with a photon energy close to that of the CO_2-laser would be preferred, in particular, to be able to cover the whole $45...500\,\mathrm{GeV}$ beam energy range of the ILC.

Acknowledgements

References

[1] V. N. Duginov et al., LC-DET-2004-031

[2] I. P. Karabekov, D. L. Egikian and C. Yang, Nucl. Instrum. Meth. A **286** (1990) 37.

[3] S. Knyazian, A.T. Margarian, S. Mehrabian, YERPHI 1486(3)-97

[4] A. H. Compton, Phys. Rev. **21** (1923) 483-502.

[5] O. Klein, Y. Nishina, Z. Phys. **52** (1929) 853.

[6] D. P. Barber et al., Nucl. Instrum. Meth. A **329** (1993) 79.

[7] C. Y. Prescott, SLAC-TN-73-001

[8] T. Suzuki, KEK-76-3

[9] G. Bardin, C. Cavata and J. P. Jorda, DESY-TESLA-97-03

[10] I. Will, G. Koss and I. Templin, Nucl. Instrum. Meth. A **541** (2005) 467.